

## Electronic Supplementary Information for

# Mechano-thermochemical synthesis of rare-earth metal-organic frameworks with solvent-free coordination for visible and near-infrared emission

Jiaqiang Liu<sup>‡a, b, c</sup>, Yifu Chen<sup>‡a, b, c</sup>, Xin Su<sup>‡a, b, c</sup> and Junbo Gong<sup>\*a, b, c</sup>

<sup>a</sup> State Key Laboratory of Chemical Engineering, School of Chemical Engineering and Technology, Tianjin University, Weijin Road 92, Tianjin, 300072, P.R. China.

<sup>b</sup> Collaborative Innovation Center of Chemistry Science and Engineering, Weijin Road 92, Tianjin, P.R. China

<sup>c</sup> Haihe Laboratory of Sustainable Chemical Transformations, Tianjin, 300192, P.R. China.

\*To whom correspondence should be sent: junbo\_gong@tju.edu.cn.

### Author Contributions

J. Liu and X. Su codesigned the experiments, implemented the preparation of materials, did characterization tests and analyzed the experimental results. Y. Chen supervised the whole study, revised the manuscript, discussed the results and helped draw figures. J. Liu, Y. Chen and X. Su contributed equally to this work. J. Gong acquired funding for the whole study. All authors commented on the manuscript.

### General Information

All sample powder X-ray diffraction (PXRD) data in this work were collected on a Rigaku D/MAX 2500 X-ray diffractometer using Cu-K $\alpha$  radiation ( $\lambda = 1.54178 \text{ \AA}$ ). The voltage and current were 40 kV and 200 mA, respectively. Powder samples used for refinement of structures were scanned in the  $2\theta$  range of  $2-90^\circ$  at a scan rate of  $2^\circ/\text{min}$ . Other powder samples were scanned in the  $2\theta$  range of  $5-65^\circ$  at a scanning speed of  $8^\circ/\text{min}$ . In situ PXRD test results were collected by varying the temperature in air from  $30^\circ\text{C}$  to  $900^\circ\text{C}$  with a  $5^\circ/\text{min}$  ramp-up.

The FTIR spectra of powders were collected by a Bruker  $\alpha$  FTIR-ATR instrument (Germany) with a resolution value of  $4 \text{ cm}^{-1}$ , scan time of 16 min, and wavenumber ranging from  $400$  to  $4000 \text{ cm}^{-1}$ . Thermogravimetric (TG) analysis was carried out on a model TGA 1/SF thermogravimetric analysis system (Mettler Toledo, Switzerland).

Photoluminescence (PL) spectra were studied on a steady/transient fluorescence spectrometer FLS 1000, equipped with a 150 W xenon lamp as excitation light source. Quantum yields were determined by the instrument equipped with an integrating sphere.

The morphologies of the samples were studied using a scanning electron microscope (SEM, Hitachi

SU-8010). The energy dispersive spectroscopy (EDS) attached to the SEM was used to examine the chemical compositions of the prepared samples.

ICP measurement: The sample TJU-66 (Yb/Sc) was dissolved in HNO<sub>3</sub> solution. The content of Yb and Sc was measured by an inductively coupled plasma-atomic emission spectrometer (Agilent 5110, USA).

### Materials and Preparation

All starting materials were obtained commercially and used without further purification.

Sc(NO<sub>3</sub>)<sub>3</sub>·xH<sub>2</sub>O (99.99%), Y(NO<sub>3</sub>)<sub>3</sub>·6H<sub>2</sub>O (99.5%), La(NO<sub>3</sub>)<sub>3</sub>·6H<sub>2</sub>O (99.9%), Ce(NO<sub>3</sub>)<sub>3</sub>·6H<sub>2</sub>O (99.9%), Pr(NO<sub>3</sub>)<sub>3</sub>·6H<sub>2</sub>O (99.9%), Nd(NO<sub>3</sub>)<sub>3</sub>·6H<sub>2</sub>O (99.9%), Sm(NO<sub>3</sub>)<sub>3</sub>·6H<sub>2</sub>O (99.9%), Eu(NO<sub>3</sub>)<sub>3</sub>·6H<sub>2</sub>O (99.9%), Gd(NO<sub>3</sub>)<sub>3</sub>·6H<sub>2</sub>O (99.9%), Tb(NO<sub>3</sub>)<sub>3</sub>·6H<sub>2</sub>O (99.9%), Dy(NO<sub>3</sub>)<sub>3</sub>·6H<sub>2</sub>O (99.99%), Ho(NO<sub>3</sub>)<sub>3</sub>·5H<sub>2</sub>O (99.9%), Er(NO<sub>3</sub>)<sub>3</sub>·6H<sub>2</sub>O (99.99%), Tm(NO<sub>3</sub>)<sub>3</sub>·5H<sub>2</sub>O (99.9%), Yb(NO<sub>3</sub>)<sub>3</sub>·5H<sub>2</sub>O (99.9%), Lu(NO<sub>3</sub>)<sub>3</sub>·6H<sub>2</sub>O (99.99%) and H<sub>3</sub>BTC (benzene-1,3,5-tricarboxylate, 98%) were purchased from Aladdin Chemical Reagent. The preparation of single- or multi-component RE-MOFs in this work was modified from a typical synthetic process. Synthesis of single-component RE-MOFs (RE=Sc, Y, La, Ce, Pr, Nd, Sm, Eu, Gd, Tb, Dy, Ho, Er, Tm, Yb or Lu): 2 mmol of rare earth nitrate, 2 mmol of H<sub>3</sub>BTC were mixed and ground in a mortar for 3 min. The mixture was then transferred to a 25 mL autoclave and heated at 140 °C for 24 hours. After cooling to room temperature, the product was collected and washed several times with distilled water and ethanol, and then dried at 60 °C for 2 h to obtain one-component RE-MOFs material. Synthesis of multicomponent RE-MOFs (RE=Nd/Sc, Sm/Sc, Eu/Sc, Tb/Sc, Dy/Sc, Er/Sc or Yb/Sc): 1 mmol each of two rare earth nitrates and 2 mmol of H<sub>3</sub>BTC were mixed and ground in a mortar for 3 min. The mixture was then transferred to a 25 mL autoclave and heated at 140 °C for 24 hours. After cooling to room temperature, the product was collected and washed several times with distilled water and ethanol, and then dried at 60 °C for 2 h to obtain the multi-component RE-MOFs material.

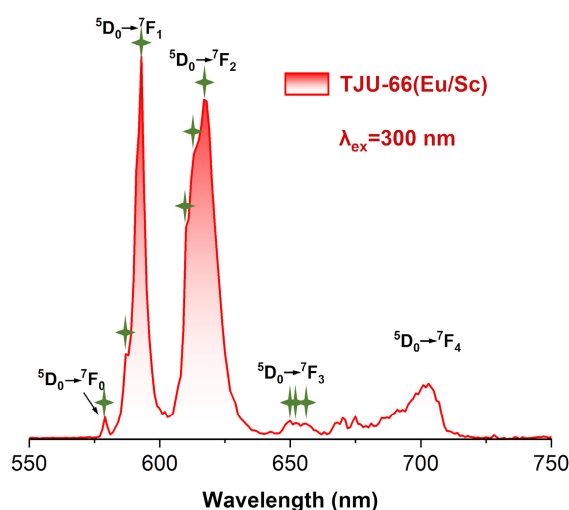


Figure S1. Photoluminescence (PL) spectrum of TJU-66 (Eu/Sc). (λ<sub>ex</sub> = 300 nm)

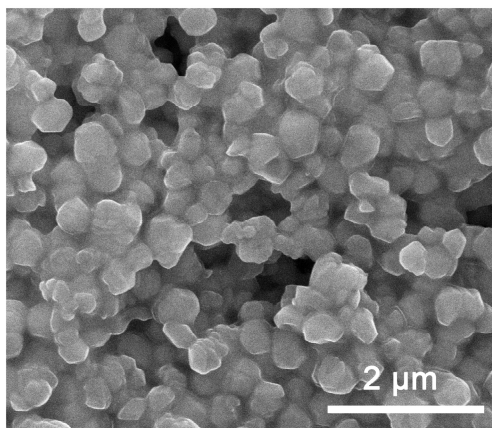


Figure S2. Scanning electron microscopy of TJU-66 (Yb).

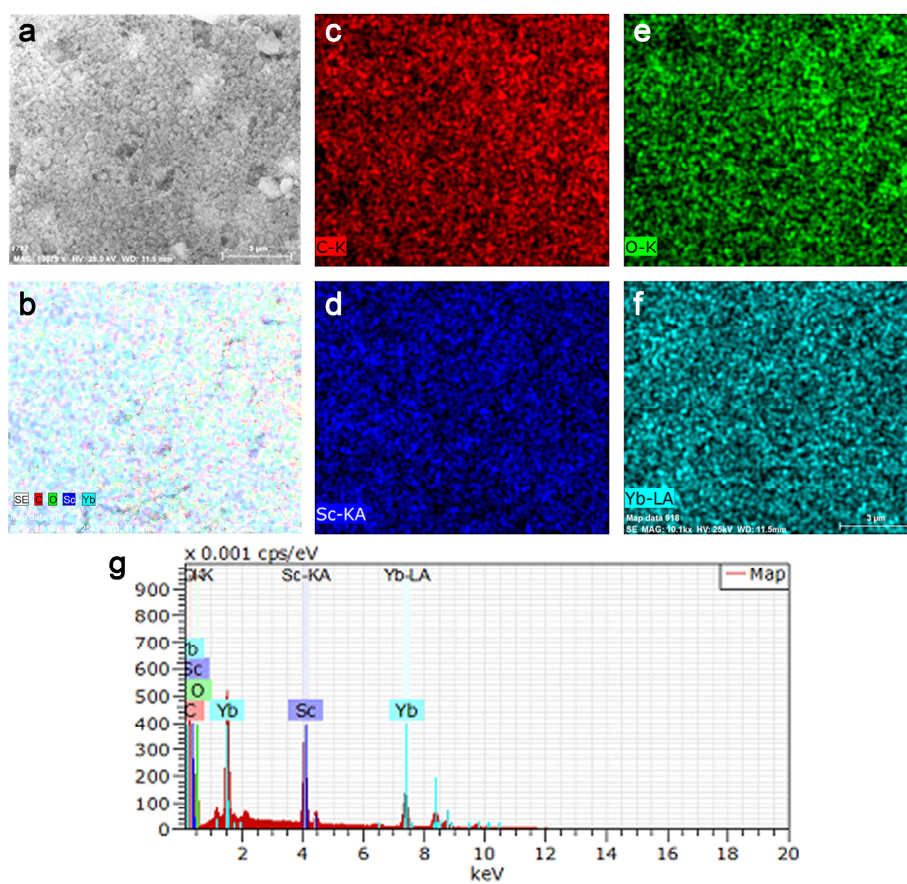


Figure S3. (a) Scanning electron microscopy image and (b) corresponding elemental mapping images with energy-dispersive X-ray spectrometry of (c) C, (d) O, (e) Sc, (f) Yb, and (g) the corresponding spectrum from TJU-66 (Yb/Sc).

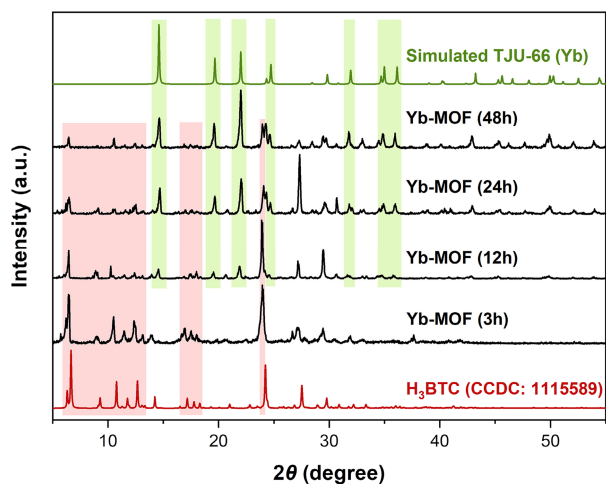


Figure S4. PXRD of synthetic TJU-66(Yb) with different heat treatment times.

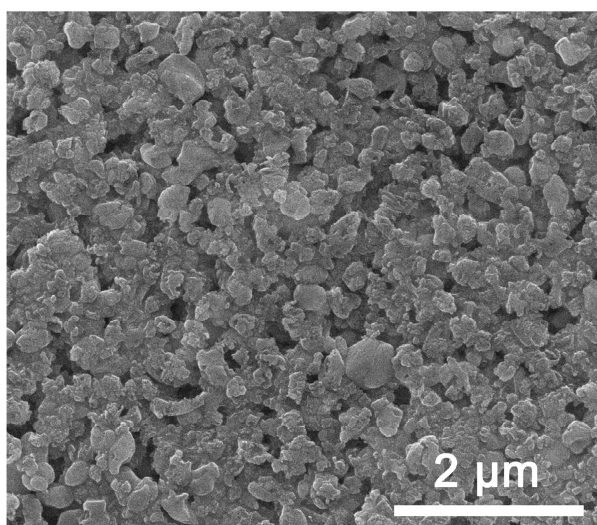


Figure S5. Scanning electron microscopy of TJU-66 (Yb/Sc).

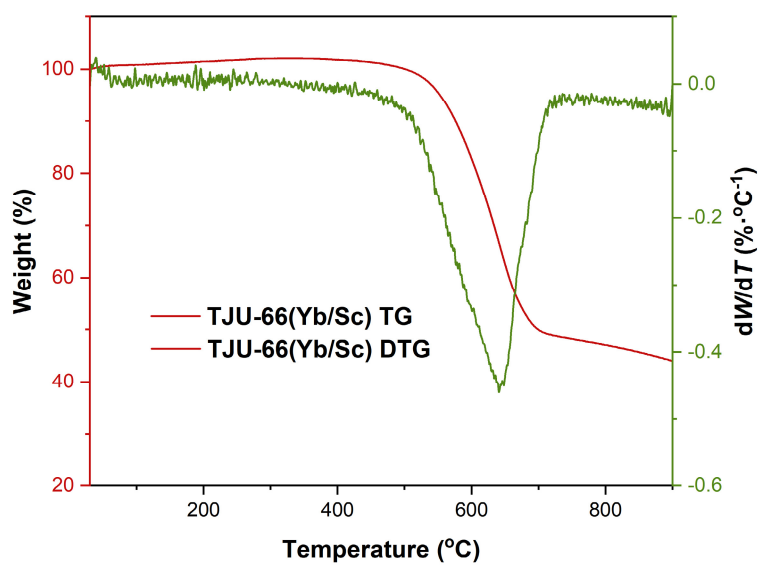


Figure S6. TGA curves registered under dynamic N<sub>2</sub> atmosphere of TJU-66(Yb/Sc).



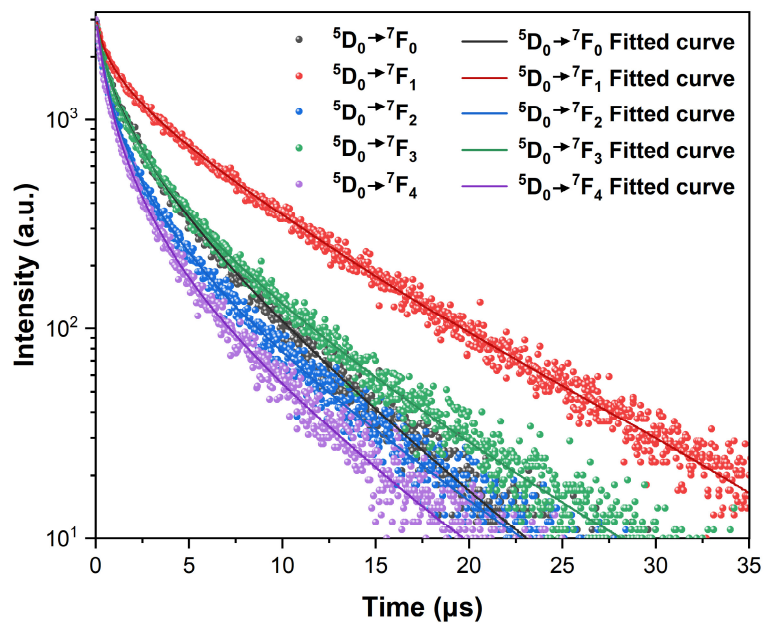


Figure S7. Fluorescence lifetimes of TJU-66 (Eu/Sc).

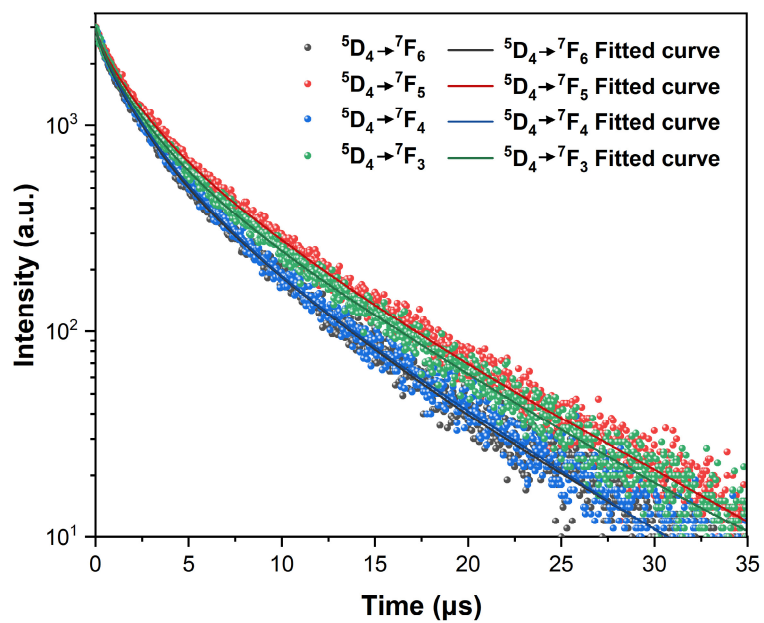


Figure S8. Fluorescence lifetimes of TJU-66 (Tb/Sc).

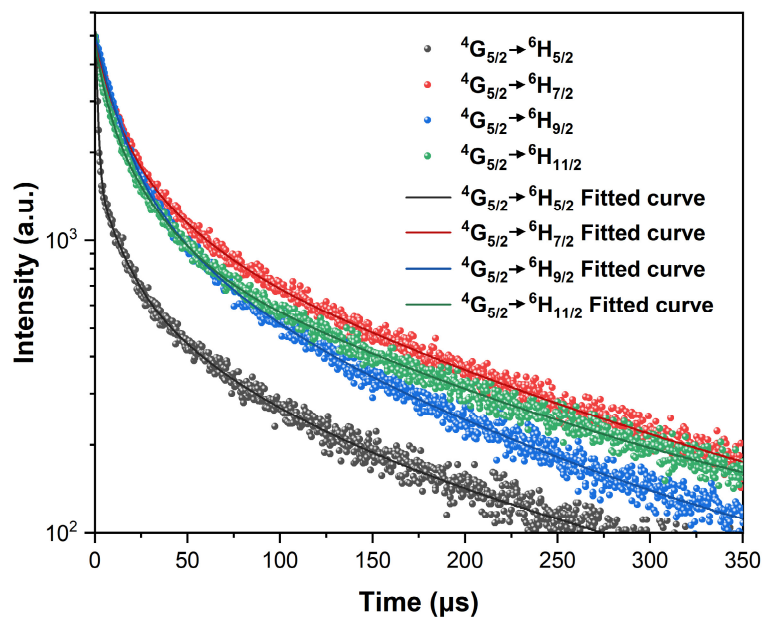


Figure S9. Fluorescence lifetimes of TJU-66 (Sm/Sc).

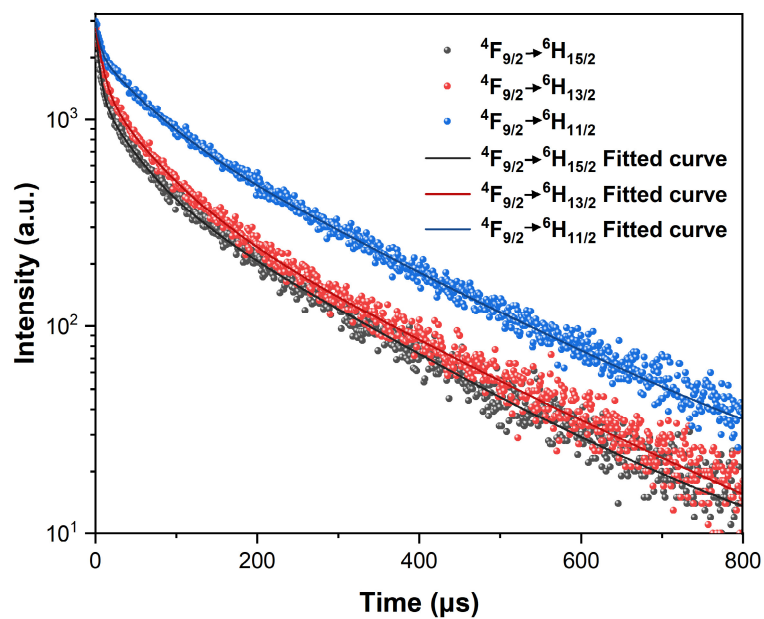


Figure S10. Fluorescence lifetimes of TJU-66 (Dy/Sc).

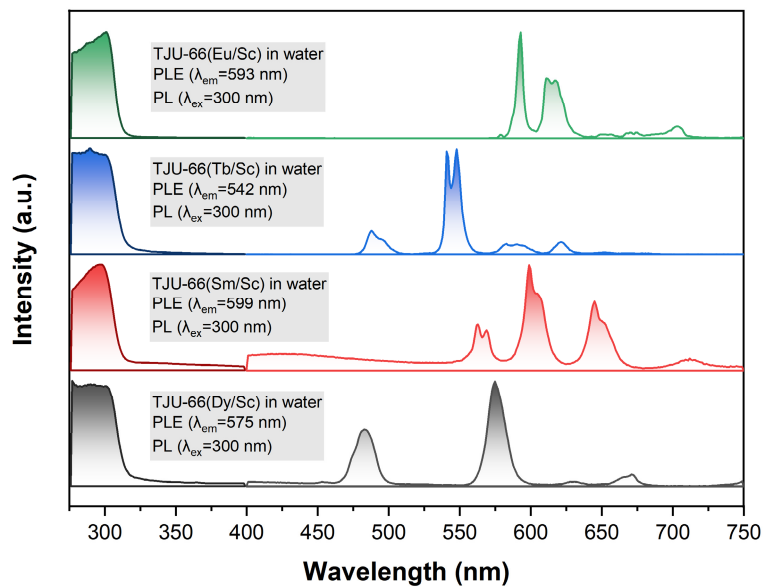


Figure S11. PLE and PL spectrum of TJU-66 (RE/Sc) (RE = Eu, Tb or Dy) in water.

Table S1 Quantum yields and luminescence lifetimes of TJU-66 (RE/Sc) (RE=Eu, Tb, Sm or Dy).<sup>a</sup>

	$Q_{Yb}^1$ (%)	Lifetime ( $\mu$ s)
TJU-66(Eu/Sc)	39.24	$^5D_0 \rightarrow ^7F_0$ $\tau_{au}$ : 3798.7(432.7)
		$^5D_0 \rightarrow ^7F_1$ $\tau_{au}$ : 7224.8(2036.9)
		$^5D_0 \rightarrow ^7F_2$ $\tau_{au}$ : 3713.8(331.0)
		$^5D_0 \rightarrow ^7F_3$ $\tau_{au}$ : 4809.6(1843.1)
		$^5D_0 \rightarrow ^7F_4$ $\tau_{au}$ : 3167.4(1016.3)
TJU-66(Tb/Sc)	32.24	$^5D_4 \rightarrow ^7F_6$ $\tau_{au}$ : 5505.2(4575.2)
		$^5D_4 \rightarrow ^7F_5$ $\tau_{au}$ : 6276.3(2876.1)
		$^5D_4 \rightarrow ^7F_4$ $\tau_{au}$ : 4858.9(363.7)
		$^5D_4 \rightarrow ^7F_3$ $\tau_{au}$ : 5585.4(283.3)
TJU-66(Sm/Sc)	2.57	$^4G_{5/2} \rightarrow ^6H_{5/2}$ $\tau_{au}$ : 1.6(0.8)
		$^4G_{5/2} \rightarrow ^6H_{7/2}$ $\tau_{au}$ : 11.5(0.6)
		$^4G_{5/2} \rightarrow ^6H_{9/2}$ $\tau_{au}$ : 8.9(0.6)
		$^4G_{5/2} \rightarrow ^6H_{11/2}$ $\tau_{au}$ : 10.6(0.4)
TJU-66(Dy/Sc)	1.71	$^4F_{9/2} \rightarrow ^6H_{15/2}$ $\tau_{au}$ : 14.7(0.3)
		$^4F_{9/2} \rightarrow ^6H_{13/2}$ $\tau_{au}$ : 15.4(0.6)
		$^4F_{9/2} \rightarrow ^6H_{11/2}$ $\tau_{au}$ : 17.8(0.3)

<sup>a</sup>Error values are given between the parentheses. Lifetimes measured under excitation at 300 nm.

Table S2 The content of Yb and Sc in TJU-66 (Yb/Sc).

Element	Sample elemental content $C_x$ (mg/kg)	Sample elemental content $W$ (%)
Sc	240610.32	24.0610%
Yb	248791.07	24.8791%

The mechanism of fluorescence lifetime enhancement:

We suggest that the lifetime improvement is due to the avoidance of concentration quenching by ion doping. Concentration quenching in Yb-based MOFs is mainly a phonon-assisted energy transfer relaxation in which the energy from a donor is directly transferred to the phonon modes of the acceptor, as shown in Figure S12. Thus, the phonon modes responsible for multiphonon relaxation are eliminated by ion doping to achieve long fluorescence lifetimes in Yb-based MOFs.<sup>1</sup>

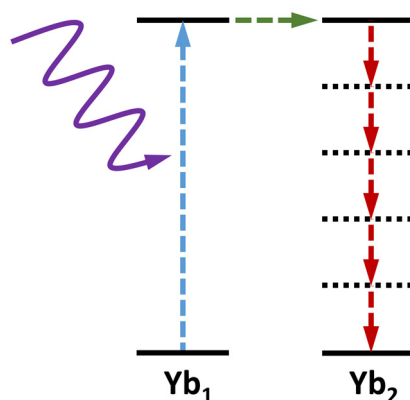


Figure S12. Phonon-assisted energy transfer relaxation. Blue arrows: excitation process, red arrows: relaxation process, green arrows: energy transfer, dotted lines: nonradiative process, and wavy arrows: photon.

## References

1. S. Omagari, T. Nakanishi, Y. Hirai, Y. Kitagawa, T. Seki, K. Fushimi, H. Ito and Y. Hasegawa, Origin of Concentration Quenching in Ytterbium Coordination Polymers: Phonon-Assisted Energy Transfer, *Eur. J. Inorg. Chem.*, **2017**, 561-567.